Evaporative Light-Scattering Detection in the Quantitative Analysis of Semivolatile Polycyclic Aromatic Compounds by High-Performance Liquid Chromatography

Vicente L. Cebolla*, Luis Membrado, Jesús Vela, and **Ana C. Ferrando**

Departamento de Procesos Químicos, Instituto de Carboquímica, CSIC, Calle Poeta Luciano Gracia, 5, 50015 Zaragoza, Spain

Abstract

Polycyclic aromatic compounds (PACs) with molecular weights lower than 300 were not considered in the past to be analyzable using an evaporative light-scattering detector (ELSD) due exclusively to their supposed volatility. We demonstrate that a variety of small, low-boiling, 3–6-ringed PACs (which include condensed PAHs, heteronuclear polycyclic compounds, and hydroxy-PAHs) can be analyzed using ELSD under mild working conditions without significant volatilization. Although area counts versus sample load can be linearized with adequate regression coefficients in the mass range studied, results obtained from the injection of pure and binary mixtures of PACs indicate that ELSD behaves nonlinearly at low sample loads, regardless of the volatility or involatility of each compound. Quite uniform response factors are obtained on the linear zone for the studied PACs, and analyses of mixtures are carried out with errors generally lower than 6%. Experimental data are better fitted to logarithmic regressions, which provide similar slopes for the studied PACs, which in turn suggest that ELSD operates in similar scattering domains for these compounds under our working conditions. The use of a mathematical simulation of particle size distributions after nebulization and evaporation confirms this and explains why response factors of PACs are similar.

Introduction

An important drawback in the high-performance liquid chromatographic (HPLC) analysis of samples containing complex mixtures of polycyclic aromatic compounds (PACs) and related compounds (e.g., fossil fuels) is quantitation using conventional detectors. This problem becomes more serious in the case of heavy fossil fuels (coal–tar pitches, heavy oils, etc.), in which unknown components are present. It is well-known that the response factors for the components in these kinds of mixtures can be very different using ultraviolet (UV) detection (1). In the same manner, responses derived from refractive index (RI) detection were found to depend on the functional groups present as well as their molecular weight (MW) (2). Although the RI detector is universal, it is less sensitive than UV, and it is incompatible with elution gradients. Likewise, flame-ionization detection (FID) for HPLC presents technical problems that cause the responses to vary due to a nonuniform deposit of the effluent (3); FID is better adapted to thin-layer chromatography (TLC) (4).

An ideal detector for chromatography of fossil fuels should give uniform response factors (no more variable than an FID for gas chromatography) for each separated compound or class of compounds.

It has been reported since the 1970s that the evaporative light-scattering detector (ELSD) enables all types of nonvolatile solutes to be detected and can be used as a mass detector over a substantial range of operating conditions and sample properties (5–10). The analysis of some semivolatile solutes that have a lower volatility than the mobile phase has been reported (11). ELSD response is quite independent of the chemical composition of the solute, so it provides reasonably uniform response factors (12). It has also been pointed out that ELSD allows for a good approximate quantitation of the constituents of a complex mixture, even if there are unknown compounds (6,13). Other advantages of this detector have been reported with respect to RI, such as the possibility of using solvent gradients, good sensitivity, and elimination of typical solvent front interferences caused by RI (14).

ELSD is and has been mostly applied to low UV-absorbant, nonvolatile solutes. Likewise, despite the relatively theoretical independence of ELSD response with regard to chemical composition, most papers in the literature refer to samples with a high degree of chemical homogeneity. ELSD has also been applied to fossil fuels since the 1980s. Pioneering work concerning the application of ELSD to products derived from fossil fuels was published in 1983 by Bartle et al. (15), in which they studied the variations of response with MW for coal extracts and their fractions. Later, Larsen et al. (16,17) applied ELSD to coal–pyridine extracts. In that work, the obtained MW distributions underestimated the amount of very low MWs present. A more recent work stressed the fact that ELSD is an adequate detector for evaluating the heaviest part of a heavy coal extract with regard to other conventional detectors (18).

The study of the chromatographic responses of PACs has

* Author to whom correspondence should be addressed.

been mainly due to their presence in coal and petroleum-derived products. Because of the complexity of these products, standards are usually studied previous to the analysis of real samples, when a chromatographic technique is to be developed. However, few systematic and detailed works can be found in the literature that deal with the viability of analyzing PACs and related compounds using ELSD.

It has been reported that the ELSD responses of PACs and other related compounds were almost uniform for MWs above 300 (15). For compounds with lower MWs, authors concluded that solutes were volatilized at work temperature (40°C). Several years later, another work (3) also questioned the analysis of different PACs and heavy oil-related compounds with MWs lower than 300. Even without heating, significant differences were obtained with regard to response factors using the nebulization technology of the time. However, response factors have been reported at a given arbitrary mass, and mostly single standards have been studied.

Given that the volatility of a compound under particular ELSD working conditions cannot be predicted merely by its boiling point or its MW (5), this work was intended to evaluate in detail the possibility of using ELSD for the chromatographic analysis of semivolatile PACs, emphasizing some of the PACs considered by Environmental Protection Agency methods (3–6 rings). The analysis of these compounds also holds relevance to coal–tar pitch characterization and environmental analysis. For this purpose, differences between area percentages from ELSD and known mass percentages for binary mixtures of PACs were evaluated, and their evolution with the mass was studied. Also, absolute response factors were determined at different masses and two evaporation temperatures.

Experimental

Chromatographic system and procedure

The solvent delivery system used in this work consisted of a Waters model 510 HPLC pump (Waters, Milford, MA). Sample injection was performed by using a 7725i Rheodyne sample injector (Rheodyne, Cotati, CA). The column was a polystyrene–divinylbenzene-based PL-Gel Mixed-E column (30 cm in length, 0.75 cm in diameter) with mixed pore distribution and 3-µm particle size (Polymer Laboratories, Shropshire, UK). GPC-grade tetrahydrofuran (THF) stabilized with 2,6-di-tert-butyl-4-methylphenol (BHT) from Scharlau (Barcelona, Spain) was used as the mobile phase. The flow rate was 1 mL/min, which was considered a good compromise for both elution and detection (10,19).

A PL-EMD 950 mass ELSD (Polymer Laboratories) was used thoughout this work. The operating mode of the detector was as follows. The effluent from the chromatographic column entered a Venturi nebulizer and was converted into aerosol by a stream of air. The Venturi consisted of a stainless steel capillary tube (0.25-mm i.d., 1.59-mm o.d.) carrying the column effluent, which was surrounded by a larger tube (2-mm i.d.). The fine droplets that were formed were then carried out through a temperature-controlled drift tube which caused evaporation of the mobile phase to form small particles of nonvolatile solute. This cloud of solute passed through a white light in the broad band 400–700 nm (generated from a tungsten light source), which produced light scattering, which in turn was detected by a photomultiplier at a 45° angle. The studied evaporation temperatures were 30 and 40°C, and the photomultiplier sensitivity used was usually 3. (Sensitivity is in arbitrary units, from 1 to 6). The output signal from the detector was fed into a Fluke Hydra 2620 multichannel data acquisition unit (Fluke Europe, Eindhoven, Netherlands) and stored in an HP 95LX computer (Hewlett-Packard, Corvallis, OR) for data acquisition. Raw data were further reprocessed using an adequate spreadsheet in a 486 PC clone.

Standards

The standards used, as well as some of their chemical and physical properties, are listed in Table I. Standards were supplied by Acros Chimica (Geel, Belgium). The properties detailed for these compounds were mainly found in the Thermodynamics Research Center database (Texas A&M University, College Station, TX).

Solutions of standards were prepared in stabilized THF. The amounts (µg) reported throughout the text correspond to the mass effectively injected. Single standards or binary mixtures of PACs were injected. In the latter case, each standard was injected together with a reference compound: coronene (CRN) or 2-hydroxycarbazole (HCBZ). The use of CRN or HCBZ as a reference compound depended on which retention time was more adequate for each particular standard. Each sample was injected at least in duplicate.

The response factor of each standard was defined as its corresponding area (counts as $\mu V \times s^{-1}$) per mass unit (µg). Only absolute response factors were used throughout this paper.

Tools for the mathematical calculations

Differential equations involved in the calculations of droplet and particle size distributions obtained after nebulization and evaporation, respectively, were solved using PSI-Plot software (Poly Software International, Salt Lake City, UT). The two methods for solving equations (fourth-order Runge-Kutta and Bulirsch-Stoer) were in agreement.

Results and Discussion

Repeatability of chromatographic analyses using ELSD

Relative standard deviations (RSDs) of analyses at the conditions used (12 L/min of air for nebulizing and 30°C for evaporating the mobile phase) were calculated (Table II). RSD is defined here as follows.

$$RSD = \sigma \times \frac{100}{\mu} \qquad \text{Eq 1}$$

where σ is the sample standard deviation, and μ is the average of the measurements.

Similar RSDs (close to 10) of the corresponding response factor were obtained at 40 µg for single compounds such as CRN or HCBZ, which are chemically different. CRN is hardly volatile at relatively high temperatures and has been considered nonvolatile in previous works (15) (Table I).

Given that the sensitivity of compounds is not the same with regard to the nebulization and evaporation conditions, the repeatability of some semivolatile compounds was tested. Thus, RSD values of response factors and area percentages were obtained for binary mixtures; each included a semivolatile PAC and a nonvolatile reference compound (either HCBZ or CRN). Table II shows the RSDs for anthracene, phenanthrene, chrysene, 2-naphthol, 9-hydroxyfluorene, and carbazole. Repeatabilities for these semivolatile compounds were, in general, lower than 10% RSD.

Chromatographic quantitation of PACs using ELSD

The main purpose of this work was to evaluate (*a*) whether ELSD truly underestimates compounds with MWs lower than

Table I. Properties of the Studied Standards

Standard	Formula	MW	Boiling point (°C)	Vapor pressure (mm Hg) at different temperatures* 30–149°C	150–199°C	>200°C
Planar, cata-PAH						
Anthracene	$C_{14}H_{10}$	178	340			44.85 (221)
Phenanthrene	$C_{14}H_{10}$	178	336	0.687 (108)		
Fluoranthene	$C_{16}H_{10}$	202	384			17.61 (220)
Crysene	$C_{18}H_{10}$	228	448	6.49×10^{-3} (100)	5.79×10^{-3} (150)	
Planar, peri-PAH						
Pyrene	$C_{16}H_{10}$	202	260†			13.79 (230)
Perylene	$C_{20}H_{12}$	252	350	3.12×10^{-6} (100)	6.21×10^{-4} (150)	
Benzo[*a*]pyrene	$C_{20}H_{12}$	252	495	8.27×10^{-4} (100)		
Coronene	$C_{24}H_{12}$	300	525		1.63×10^{-5} (150)	0.019 (245)
Non-planar PAH						
Acenaphthene	$C_{12}H_{10}$	154	279	3.371 (105)		
Fluorene	$C_{13}H_{10}$	166	298	3.592 (119)		
1,2-Dihydronaphthalene	$C_{10}H_{10}$	130	89			
2,3-Benzofluorene	$C_{17}H_{12}$	216	—			
Alkyl-PAH						
2-Methylnaphthalene	$C_{11}H_{10}$	142	241	44.1 (141)	288.3 (200)	920.3 (250)
Hydroxy-PAC						
2-Naphthol	$C_{10}H_8O$	144	285		11.1 (150)	137.2 (220)
9-Hydroxyfluorene	$C_{13}H_{10}O$	182				
9-Phenanthrol	$C_{14}H_{10}O$	194				
***N*-Heterocycles**						
Carbazole	$C_{12}H_9N$	167	355			71.42 (220)
2-Hydroxycarbazole	$C_{12}H_9NO$	183				
Acridine	$C_{13}H_9N$	179	346	0.459 (115)	2.538 (150)	34.63 (220)
7,8-Benzoquinoline	$C_{13}H_9N$	179	338‡	3.93×10^{-4} (30)		
***O*-Heterocycles**						
Dibenzofuran	$C_{12}H_8O$	168	155§	6.44 (120)	80.51 (190)	233.7 (230)
***N,O*-Heterocycles**						
Phenoxazine	$C_{12}H_9NO$	183				
***S*-Compounds**						
Dibenzothiophene	$C_{12}H_8S$	184	333			
Phenyldisulfide	$C_{12}H_{10}S$	218				
Tianthrene	$C_{12}H_8S_2$	216	366			

* Ranges of temperature (°C) studied for each standard: anthracene, 221; phenanthrene, 108; fluoranthene, 220; crysene, 75–200; pyrene, 230; perylene, 100–190; benzo[*a*]pyrene, 75–168; coronene, 144–247; acenaphthene, 105; fluorene, 119; 2-methylnaphthalene, 140–252; 2-naphthol, 144–308; carbazole, 253–358; acridine, 115–360; 7,8-benzoquinoline, 20–50; dibenzofuran, 120–296. Between parentheses, temperature at which the vapor pressure is given (°C).
† at 60 mm Hg.
‡ at 719 mm Hg.
§ at 20 mm Hg.

300, and (*b*) whether ELSD can effectively be considered a mass detector for the analysis of the compounds studied. In other words, we intended to evaluate whether area percentages of peaks in mixtures are equal to mass percentages that are injected so that we could avoid previous calibration. In the first step of the research, samples that corresponded to different amounts of a binary mixture of HCBZ (5–50 µg) and CRN (5–50 µg) were injected. Differences between the obtained area percentages from ELSD and the known mass percentages (hereafter referred to as *A–m* differences) were evaluated as a function of the amount injected and as a function of the absolute response factors. HCBZ and CRN were chosen due to their different physical and chemical properties and very low volatility at working conditions (Table I).

When area counts (*A*) versus sample mass injected (*m*) for a given compound can be linearized with adequate regression coefficients, the slope of the regression represents the theoretical response factor (*A/m*) of the compound. In the case of an ideal linear detector, the response factor should be constant, regardless of the mass injected. Moreover, between the detectors commonly considered as linear, slopes vary for each different compound to an extent that depends on each particular detection system. If an ideal detector existed for which the slopes of all the detected compounds were equal, it would be a true mass detector.

Table III shows that the lower the amount injected (for each component of the mixture), the greater the *A–m* difference. This was lower than 1.5% for the amounts greater than 40 µg. (It must be remembered that each sample was injected in duplicate, and results were always within 1.7% of the area percentage for 99% of the confidence level.) Obviously, the evolution of *A–m* differences for different sample loads was also reflected in the evolution of the response factor ratio between the mixture components. Likewise, significantly lower response factor values were found in the cases of lower masses. As the amount injected increased (see Table III), the response factors for both HCBZ and CRN progressively increased, and relative differences between them were progressively smaller. Thus, the estimated response factors at 40 µg were quite similar for HCBZ and CRN.

Table II. RSD of Chromatographic Analyses of Single Compounds (40 µg) and Binary Mixtures (40 µg of Each Component) Using ELSD at 30°C

	No. of samples	RSD% of area%	RSD% of *A/m*
2-Hydroxycarbazole*	19	–	9.3
Coronene*	14	–	9.8
Anthracene	5	6.5	9.2
2-Hydroxycarbazole		6.1	9.9
Phenanthrene	5	6.0	6.7
2-Hydroxycarbazole		4.2	3.0
Chrysene	3	8.0	5.9
2-Hydroxycarbazole		4.4	5.1
2-Naphthol	4	7.7	11.5
Coronene		9.7	10.3
9-Hydroxyfluorene	3	1.6	3.4
Coronene		2.1	3.9
Carbazole	3	4.3	9.6
Coronene		6.0	10.6

* Single compound.

Table III. Evolution in Function of Injected Mass, Response Factors (*A/m*), and Area Percentages from ELSD (30°C) of a Mixture Containing HCBZ and CRN

Mass injected (µg)*		Mass %	Area %	*A/m*
5	HCBZ	57.4	68.2	0.790
	CRN	42.6	31.8	0.495
20	HCBZ	55.5	63.7	1.220
	CRN	44.5	36.3	0.870
30	HCBZ	50.6	56.0	1.17
	CRN	49.4	44.0	0.942
40	HCBZ	46.4	47.9	1.390
	CRN	53.6	52.1	1.308
50	HCBZ	50.0	50.1	1.404
	CRN	50.0	49.9	1.400

* Of each component.

The above-mentioned response factor values at the lowest masses suggested a deviation of ELSD from linearity, although results can be linearized with adequate regression coefficients (Table IV). Results similar to those found in this work were recently reported by Dreux et al. (11) concerning detection of glucose on an octadecyl bonded-silica column; pure water was the mobile phase, and either ELSD or RI detection was used. This work demonstrated large deviations from linearity for both detectors at low sample loads despite good regression coefficients. Even larger deviations were found for RI detection than for ELSD; the former is usually considered to be a linear detector. Data were much better fitted to a logarithmic regression: $\log A = b \log m + \log a$, from $A = a\, m^b$, where *a* and *b* are ELSD coefficients that depend on the nebulization and evaporation conditions, chromatographic system, and the concentration and some properties of the solute. This expression is general and is applied to any detection system in which *a* and *b* are constants of each particular detection system (20). According to this, no detector has been manufactured so far that has a value of *b* equal to 1 over more than two orders of the concentration range. In LC, detectors rarely have *b* values between 0.98 and 1.02 over a range much greater than 3 orders of magnitude. From the point of view of quantitative accuracy, *b* values do not have to be equal or close to 1 as long as an accurate value of *b* is known (20).

Theoretical values of *b* between 0.66 and 2 have been reported for ELSD (11). This is because ELSD presents different sensitivities with regard to the scattering domain of work (reflexion–refraction, Mie, and Rayleigh). These domains are determined by the ratio of a characteristic dimension (i.e.,

diameter, d_s) of the solute particle to the wavelength of the incident light beam (λ). It is very important to work in similar d_s/λ ranges in order to have homogeneous response factors for the components of a complex mixture. Rayleigh scattering is predominant when d_s/λ values are smaller than 0.1. In this domain, the intensity (I) of Rayleigh scattering depends on d_s^6, among other parameters. In general, I is a complex function not only of d_s, but of λ, n_s (refractive index of solute), polarization of the light source, collection angle, and aperture of the detector. Despite the above-mentioned dependence on diameter, I values for particles within the Rayleigh domain are lower (several orders of magnitude) than for other domains (21). Mie scattering becomes preponderant when d_s/λ is greater than 0.1. In this domain, I depends on the fourth power of the diameter. For greater d_s/λ ratios (approximately 2), reflexion and refraction become dominant and sensitivity increases. (I is a function of diameter squared). Regardless of the diameter dependence of I within each scattering domain, I values generally increase with particle size. I values from spherical particles can be calculated for any size using Mie's theory (22).

In ELSD, the diameter of solute particles after evaporating (d_s) can be related to the concentration (C) through the following equation:

$$d_s = d_m \left(\frac{C}{\rho_s}\right)^{1/3} \qquad \text{Eq 2}$$

where ρ_s is the solute density, and d_m is the droplet diameter after nebulization, which depends on the mobile phase properties and flow rate, nebulizer geometry, and nebulization conditions (10). Therefore, when I is expressed as a function of the concentration (23), $I = f(C^2)$, $f(C^{1.33})$, or $f(C^{0.66})$ for Rayleigh, Mie, or reflexion–refraction domains, respectively. Thus, ELSD response is not linear regardless of the volatility or nonvolatility of the compounds. Likewise, homogeneity in response factors for different solutes is determined to some extent for some solute properties (mostly ρ_s) and nebulization and chromatographic conditions.

Table IV presents results for some studied PACs. It shows linear and logarithmic regressions for CRN, HCBZ, and chrysene. In the case of linear regressions, error (E) was calculated in this table for each experimental point as follows:

$$E = \left[\frac{(A - A_c)}{A}\right] \times 100 \qquad \text{Eq 3}$$

In the case of logarithmic regressions, error was calculated as follows:

Table IV. Fitting of Experimental Data to Linear and Logarithmic Regressions for HCBZ, CRN, and Chrysene

Sample	Linear regression			Logarithmic regression		
Mass (m) (μg)	A	A_c*	E%†	log A	(log A)‡	E%†
HCBZ		$A = 1.542m - 6.887$ ($r = 0.9995$)			$\log A = 1.291 \times \log m - 0.340$ ($r = 0.9984$)	
7.8	6.1610	5.1387	16.59	0.7897	0.8122	−2.85
23.0	28.3028	28.5727	−0.95	1.4518	1.4185	2.29
27.0	32.9721	34.7395	−5.36	1.5181	1.5086	0.63
40.0	55.5859	54.7818	1.45	1.7450	1.729	0.92
50.0	70.1714	70.1989	−0.04	1.8462	1.8542	−0.43
63.6	91.4047	91.1662	0.26	1.9610	1.9891	−1.43
COR		$A = 1.537m - 10.070$ ($r = 0.9923$)			$\log A = 1.474 \times \log m - 0.668$ ($r = 0.9999$)	
5.8	2.8687	−1.154	140.23	0.4577	0.4575	0.04
18.4	16.0004	18.2182	−13.86	1.2041	1.1905	1.13
26.4	26.0343	30.5177	−17.22	1.4155	1.4276	−0.85
46.2	60.4614	60.9591	−0.82	1.7815	1.7858	−0.24
50.0	69.978	66.8013	4.54	1.845	1.8365	0.46
CRS		$A = 0.9940m - 3.65$ ($r = 0.9990$)			$\log A = 1.343 \times \log m - 0.59$ ($r = 0.9962$)	
4.1	1.6233	0.4083	74.85	0.2104	0.2325	−10.5
5.5	2.7594	1.8561	32.74	0.4408	0.4102	6.94
7.3	3.2515	3.5741	−9.92	0.5121	0.5685	−11.01
9.6	4.8673	5.9253	−21.74	0.6873	0.7328	−6.62
11.5	7.7914	7.8242	−0.42	0.8916	0.8383	5.98
15.4	11.4256	11.6221	−1.72	1.0579	1.0051	4.99
18.5	13.6113	14.6965	−7.97	1.1339	1.1121	1.92
35.6	32.1152	31.7872	1.02	1.5067	1.4963	0.69
57.5	53.7382	53.4893	0.46	1.7303	1.7751	−2.59

* Calculated using the corresponding linear regression equation.
† Error % according to Equations 3 and 4.
‡ Calculated using the corresponding logarithmic regression equation.

$$E = [\frac{(\log A - [\log A]_c)}{\log A}] \times 100 \qquad \text{Eq 4}$$

where A_c and $(\log A)_c$ are the values of A and $\log A$, calculated using the corresponding fitting curve.

It can be seen from Table IV that both linear and logarithmic regressions showed adequate regression coefficients (r), although logarithmic regressions provided lower errors at low sample loads. In addition, intercepts from logarithmic regressions were nearer to zero than those from linear ones. Therefore, intercepts from logarithmic regressions have more physical meaning than intercepts from linear regressions. Moreover, values of b (slopes of logarithmic regressions) were quite close for CRN, HCBZ, and chrysene, despite having different chemical natures (an N-PAC and two PAHs). Furthermore, b values were near the theoretical exponent corresponding to the Mie domain. In order to demonstrate that the diameters of PAC particles are effectively in similar domains under the chromatographic and nebulization conditions used, a mathematical simulation, presented later in this work, was carried out to calculate particle size distributions.

Other binary mixtures containing a PAC and either HCBZ or CRN as a reference were studied apart from the above-mentioned case of HCBZ and CRN mixtures. Table V shows A–m differences for 20 mixtures as well as response factors for each PAC and its corresponding reference at different sample loads (20 and 40 µg). This table also gives the response factors for the studied PACs at 8 µg.

As expected, significantly lower response factors for lower masses were obtained for each studied compound, which confirmed a deviation from linearity of ELSD at the lowest masses, regardless of the studied standard. However, the evolution of A–m differences with the mass is not the same for all the standards and depends on each particular one. In other words, the nonlinearity pattern of A–m data at low sample loads is different for the studied compounds. This is particularly important for some standards, such as phenanthrene, 7,8-benzoquinoline, dibenzothiophene, and diphenyldisulfide, which presented high A–m differences when a 20-µg sample load was used (Table V).

Results from Table V (at 40 µg, in the linear zone of ELSD) show that most of the 3–6-ringed semivolatile PAHs studied, such as anthracene, fluoranthene, 2,3-benzofluorene, pyrene, perylene, benzo[a]pyrene, and CRN, can be analyzed using ELSD under the described conditions; differences between mass and area percentages were generally lower than 6% (w/w). The same can be said for other analyzed PACs (HCBZ, acridine, 7,8-benzoquinoline, phenoxazine, diphenyldisulfide, tianthrene, 9-phenanthrol, and 2-naphthol). All these standards presented quite uniform absolute response factors despite their different chemical nature. This means that the studied PACs were not significantly volatilized under the mild conditions used despite having MWs lower than 300 and boiling points lower than 285°C. Small N-heteronuclear PACs and hydroxy-PACs presented more similar response factors than nonvolatile CRN.

Boiling point and MW are not the only properties to consider with regard to the volatility of samples. This is illustrated by the

Table V. Response Factors (A/m) and A–m Differences (Δ) of PAC Standards in Binary Mixtures at Several Sample Loads Using Either HCBZ or CRN as References

	40 µg			20 µg			8 µg
Standard	Δ*	A/m	A/m†	Δ*	A/m	A/m†	A/m§
7,8-Benzoquinoline	0.8	1.188	1.226	15.7	0.475	0.908	0.213
Diphenyldisulfide	1.0	1.187	1.227‡	7.0	0.621	0.821‡	0.347
2-Hydroxycarbazole	1.5	1.390	1.308‡	8.2	1.220	0.870‡	0.565
Coronene	1.5	1.308	1.390	8.2	0.870	1.220	0.321
Perylene	1.5	1.383	1.303	7.2	0.754	1.010	0.410
Benzo[a]pyrene	2.5	1.407	1.273	5.2	0.794	0.979	0.435
Tianthrene	2.5	1.291	1.272	1.3	0.974	0.924	0.446
Anthracene	2.6	1.002	1.113	7.0	0.733	0.972	0.536
Acridine	2.6	1.523	1.380	4.7	1.138	0.942	0.319
Phenoxazine	3.4	1.584	1.381‡	10.1	0.994	0.639‡	0.562
2-Naphthol	4.2	1.301	1.150‡	3.4	0.782	0.749‡	0.243
9-Phenanthrol	4.4	1.090	1.300‡	1.7	1.166	1.096‡	0.573
Pyrene	4.7	1.478	1.223	5.1	1.147	0.922	0.563
Fluoranthene	5.8	1.436	1.133	6.5	0.941	1.227	0.390
2,3-Benzofluorene	6.1	0.850	1.178	8.3	0.638	0.906	0.320
9-Hydroxyfluorene	6.7	1.454	1.109‡	5.8	1.083	0.883‡	0.550
Carbazole	8.7	0.917	1.305‡	7.6	0.634	0.843‡	0.389
Phenanthrene	9.0	0.775	1.116	22.2	0.419	1.093	0.225
Chrysene	9.7	0.857	1.288	9.2	0.647	0.938	0.345
Dibenzothiophene	12.4	0.866	1.444	24.4	0.290	0.813	0.109

* A–m differences in absolute value.
† Response factors of the corresponding reference compound in each experiment.
‡ Indicates A/m of CRN; the remaining refer to HCBZ.
§ Injection of single standards.

fact that, although acenaphthene and 2-naphthol have similar boiling points and MWs, acenaphthene showed no signal, whereas 2-naphthol gave a high response factor. Likewise, the simple introduction of a hydroxy group in a molecule can sometimes increase the response factor (e.g., naphthalene, which gave no signal, and 2-naphthol; carbazole and HCBZ; fluorene, which hardly gave any signal, and 9-hydroxyfluorene). According to Charlesworth (5), the relative volatilities of solutes can be assessed by comparing the temperatures at which a vapor pressure of 1 mm Hg is achieved. Given that these data are not available for many PACs, some data about vapor pressures at different temperatures for the studied PACs are given in Table I. Because of the different range of temperatures studied in each case, similar temperatures were chosen as far as possible in order to carry out relative comparisons between the most studied PACs. However, relative comparisons should be taken with caution due to the different evaporation conditions compared: evaporation at 30°C in an air stream (ELSD) and evaporation at temperatures higher than 100°C (literature data).

Although most analytes are less volatile than HPLC mobile phases, ELSD does not provide a universal response. Thus, there must be a value of vapor pressure for a given temperature over which PACs cannot be analyzed using ELSD, even under mild conditions. Two-ringed PACs (naphthalene and 2-methylnaphthalene); small, nonplanar, hydrogenated PACs (acenaphthene and fluorene); and *O*-heterocyclic dibenzofuran showed either no signal or an important loss of response at 30°C, as expected from their higher vapor pressures (Table I), compared with those of the compounds given in Table V.

2-Naphthol had the highest relative volatility (Table I) from among the analyzable compounds; *A–m* differences were lower than 6% (Table V). Likewise, phenanthrene, which had a 9% *A–m* difference, had a high relative volatility. Unfortunately, vapor pressures for both compounds were not estimated at the same temperature. This may allow the establishment of a maximum value of vapor pressure to discriminate between analyzable and nonanalyzable compounds for a given *A–m* difference.

As mentioned in the introduction, very different response factors for PACs were reported in the literature. Therefore, the impossibility of analyzing PACs by using ELSD was exclusively attributed to the supposed volatility of these compounds. Although this should not be discarded in some cases, the results presented here suggest that the values of the corresponding response factors reported in the literature were estimated at low loads and at temperatures higher than those used here. Also, there have been changes in the configuration of nebulizers in the newer models with respect to the older ones. As previously mentioned, nebulization directly influences particle diameter, which in turn affects the sensitivity of ELSD for different solutes. Figure 1 shows the different response loss of several studied compounds with an increase in the temperature setting (from 30 to 40°C). The important response loss of the studied sulfur compounds with this increase in temperature is important to note.

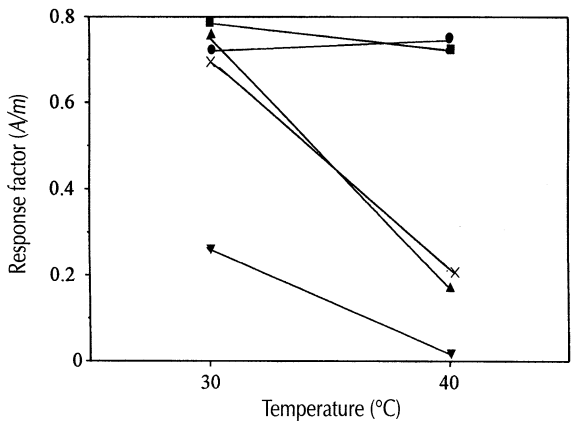

Figure 1. Response loss of some PACs with an increase in temperature setting. 20-µg sample load; photomultiplier sensitivity, 4. ■ = benzo[*a*]pyrene; ▲ = acridine; ● = 2,3-benzofluorene; × = diphenyldisulfide; ▼ = dibenzotiophene.

Mathematical calculations of droplet and particle size distributions

In this section, theoretical calculations demonstrate that PACs present similar distributions of d_s/λ values and, therefore, similar responses under our working conditions. Also, there is an agreement between experimental and theoretical data because *b* values (experimental) and d_s/λ values (theoretical) suggest similar scattering working domains for the studied PACs. Calculations of particle size distributions imply simulation of both nebulization and evaporation steps.

Nebulization

Simulation of nebulization is performed using the droplet size distribution of Mugele and Evans (10,24):

$$\frac{dn}{dd_m} = Y\frac{\delta\, d_{max}}{\sqrt{\pi}(d_{max}-d_m)}e^{\left[-\delta\left(\ln\left(\frac{a\,d_m}{d_{max}-d_m}\right)\right)+\left(\frac{1.5}{\delta}\right)\right]^2} \quad \text{Eq 5}$$

where dn/dd_m is the number of droplets with diameter d_m created per unit of time, and d_m represents the diameter of the effluent droplets. Details of the calculations, such as the values of *a* and δ constants, which depend on the nebulizer geometry, were performed as reported by Van der Meeren et al. (10). *Y* is a normalization factor, and d_{max} is the maximum diameter of the distribution:

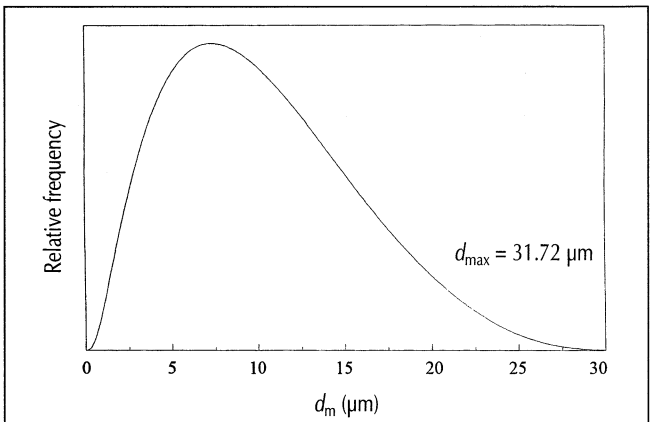

Figure 2. Droplet size distribution (in volume) from the nebulization of the chromatographic effluent in a Venturi.

$$d_{max} = d_{sv}\ (1 + a\ \exp(\frac{1}{4\delta^2}))$$ Eq 6

where d_{sv} is the surface volume mean diameter. This parameter is calculated from the Nukiyama and Tanassawa equation (10), which depends on the mobile phase properties according to the following:

$$d_{sv} = 0.585\frac{\sqrt{\pi}}{(V_g - V_l)\sqrt{\rho_m}} + 53.22[\frac{\mu}{(\sigma\rho_m)^{0.5}}]^{0.45}[\frac{Q_l}{Q_g}]^{1.5}$$ Eq 7

where σ, ρ_m, and μ are the surface tension (26.5×10^{-3} N m^{-1}), density (888 kg m^{-3}), and viscosity (4.6×10^{-4} Pa s) of the mobile phase (THF), respectively. Q is the volumetric flow rate (m^3 s^{-1}), and v is the linear velocity (m s^{-1}). Subscripts g and l refer respectively to the carrier gas and mobile phase. As indicated by Van der Meeren et al. (10), linear velocities were derived from the volumetric flow rate divided by the cross-sectional area, according to the dimensions of the Venturi. Our system meets the requirements for the application of Equation 8 with regard to physical properties of the solvent and d_{sv}, as reported by Righezza and Guiochon (25).

In our case, values for d_{sv} and d_{max} were 19.15 and 31.72 µm, respectively. In order to solve Equation 5, the diameter was discretely increased in steps of 0.1×10^{-7} m. Thus,

$$n_i = \frac{dn}{dd_m}0.1 \times 10^{-7}$$ Eq 8

The Y value in the Mugele and Evans equation was calculated from the boundary condition that the integrated volume distribution ($V_i = n_i\ [\pi d_m^3/6]$) over a unit of time must equalize the flow rate. In this way, the volume droplet size distribution after nebulization was obtained for our system (Figure 2).

Evaporation

After evaporation, the diameter of the resulting particles (d_s) depends on the diameter of the incoming droplet (d_m), solute concentration (C), and solute density (ρ_s) through Equation 2. According to this, for a given set of experimental conditions, there is no change in the number of droplets, but merely a change in their diameter. This hypothesis has generally been accepted and seems realistic in the working conditions of ELSD.

Solute concentration depends on sample load (X), time (t), and chromatographic conditions according to Equation 9:

$$C = \frac{X/10^9}{Q_l}\frac{\exp[-(t_r - t)^2/(2\,SD^2)]}{(2\pi)^{1/2}SD}$$ Eq 9

where SD and t_r are the standard deviation and retention time of the chromatographic peak, respectively. Peak width at half peak height ($W_{1/2}$) is related to SD, according to the following:

$$SD = \frac{W_{1/2}}{2\,(\ln 4)^{1/2}} = \frac{W_{1/2}}{2.35482}$$ Eq 10

Peak width depends to some extent on the retention time for a given column. However, this parameter is very similar for the studied PACs in our case because they elute within a small interval of retention time using the PL-Gel mixed E column. Calculations demonstrated that its influence on the variation of particle size was very small here.

Particle size distributions (in number and volume) were calculated for different studied PACs. For a given compound and wavelength, the intensity of scattered light is the summation of the scattered intensities produced by every particle from every particle size distribution for all time intervals considered throughout the chromatographic peak. Theoretically, the total intensity will be obtained by integrating the intensities over the wavelengths used. It should be remembered that a multiwavelength source (400–700 nm) was used throughout this work. It is important to note that, for particles of a given diameter, the working domain of ELSD will pass progressively from Mie to Rayleigh or from reflexion–refraction to Mie as the wavelength increases. Therefore, the limit between Rayleigh and Mie will depend on the considered wavelength (from 0.04 µm for a wavelength of 400 nm to 0.07 µm for a wavelength of 700 nm). In the same manner, the limit between Mie and reflexion–

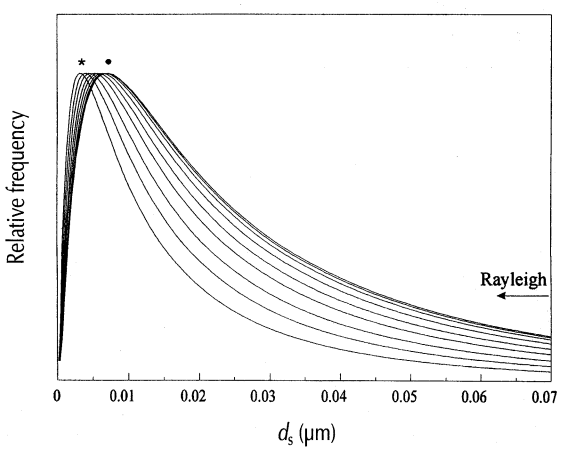

Figure 3. Nine particle size distributions (in number) corresponding to chrysene elution (5-µg load) from the start (*) of the chromatographic peak to the maximum (●) of the chromatographic peak ($t = t_r$).

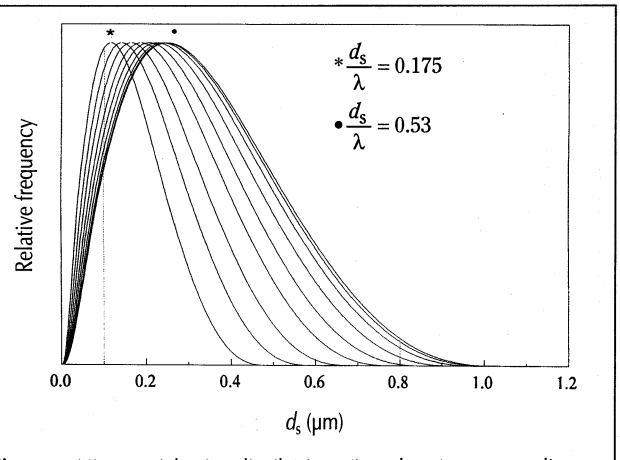

Figure 4. Nine particle size distributions (in volume) corresponding to chrysene elution (5-µg load) from the start (*) of the chromatographic peak to the maximum (●) of the chromatographic peak ($t = t_r$). Values of d_s/λ for a wavelength of 400 nm.

refraction will be from 0.8 µm for a wavelength of 400 nm to 1.4 µm for a wavelength of 700 nm.

In order to perform the calculations, peaks were assumed to be Gaussian. According to Equation 9, the particle size distribution corresponding to the maximum of the chromatographic peak ($t_r - t = 0$) presents the highest diameters. Therefore, several size distributions (nine, corresponding to eight time intervals) only along the first half of each chromatographic peak were considered. (The second half of the peak presents the same size distributions.) Figure 3 shows nine size–number distributions for the chrysene peak (5-µg sample load), and Figure 4 shows their corresponding size–volume distributions. It can be seen from these figures that most particles are in the Rayleigh domain, although a far lower number of particles in the Mie domain make the greatest contribution to volume. As previously mentioned in this work and reported in the literature (21), particles in the Mie domain mainly contribute to total intensity of light scattering with regard to those in the Rayleigh domain. Figure 4 also includes d_s/λ values for size distributions corresponding to the start and maximum of the chrysene peak. At the sample load used (5 µg), the quasi-totality of the particles presented d_s/λ values lower than 2 (reflexion–refraction), even when a wavelength of 400 nm was used for the calculations. However, sample load (X) influences particle size (d_s) through solute concentration, according to Equation 9. Figure 5 shows size–volume distributions corresponding to the maxima of the chromatographic peaks for different chrysene loads (5, 20, and 40 µg). Lower sample loads imply lower diameters and, hence, a higher proportion of particles in the Rayleigh domain. This could explain the nonlinearity of ELSD at low sample loads, although quantitative confirmation should be performed by calculating total intensities from Mie's theory (21).

Nevertheless, for a given sample load and working conditions, particle size distributions for the studied PACs are similar because their densities are not very different. As an illustrative example, Figure 6 shows similar particle size distributions at the maxima of each corresponding chromatographic peak for chrysene (ρ_s = 1274 kg m^{-3}) and CRN (ρ_s = 1371 kg m^{-3}). This explains the homogeneous response of both compounds. Moreover, it can be seen in Table IV that the experimentally obtained b values for chrysene and CRN are 1.34 and 1.47, respectively. These experimental values are near the theoretical value for the Mie domain (1.33). Calculations of d_s/λ values from particle size distributions are in agreement with this. According to Figure 6, taking into account the diameters involved in the other distributions along each chromatographic peak, a substantial proportion of particles are mainly in the Mie domain.

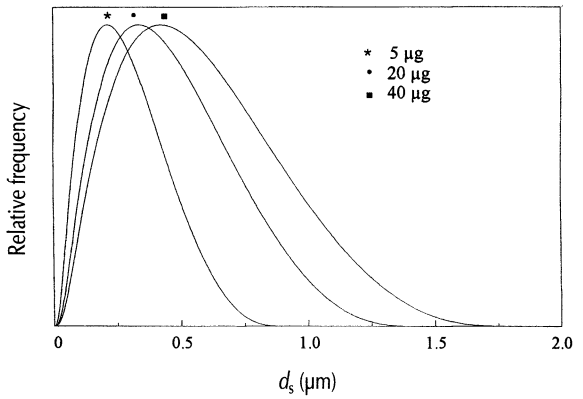

Figure 5. Particle size distributions (in volume) corresponding to the maxima of chromatographic peaks for different chrysene loads.

Conclusion

Small PACs were not considered in the past to be analyzable using ELSD due exclusively to their volatility. Although there must be a value of vapor pressure for a given temperature over which PACs cannot be analyzed using this detector (approximately corresponding to 2-ringed molecules), a variety of 3–6-ringed PACs with very different chemical natures were quantitatively determined using mild and adequate working conditions.

ELSD is usually compared to RI detection and, like the latter, shows a nonlinear behavior at low sample loads, although area counts versus sample load can be linearized in the whole mass range studied with adequate regression coefficients. Data are better fitted to a logarithmic regression.

Therefore, at low sample loads, ELSD needs a calibration step and can be useful for mixtures of known PACs in the same manner as an RI detector. However, on the linear zone of ELSD, similar response factors were obtained for chemically different PACs, unlike other conventional detectors. Thus, ELSD can be used for the analysis of complex mixtures of PACs in which there are unknown components, avoiding any calibration step.

The slopes of logarithmic regressions give information about the scattering working domains for each solute, which define the sensitivity ranges of ELSD. Thus, quantitative working conditions can be found for very different solutes as a function of their differences in density and nebulization and chromatographic conditions. In our case, response factors of PACs are similar because their densities are similar, and working conditions were adequate. Under the conditions used, PACs present d_s/λ values mainly in the Mie scattering domain.

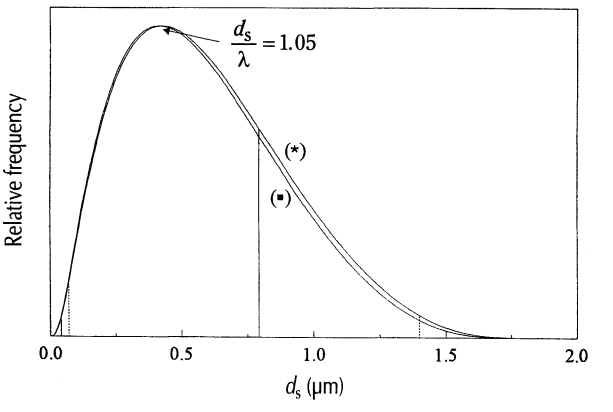

Figure 6. Particle size distributions at the maxima of the chromatographic peaks for chrysene (*) and CRN (■) (40-µg load). Continuous lines delimit Rayleigh and Mie zones for a wavelength of 400 nm, and dashed lines delimit Rayleigh and Mie zones for a wavelength of 700 nm.

Acknowledgments

The authors are grateful to Spanish DGICYT (project PB93-0100) and ECSC (European Coal & Steel Community, project 7220-EC/765) for their financial support. We also wish to thank M.J. Gayán for her technical assistance. A previous oral presentation of a summary of this work was presented before the Fuel Division of the American Chemical Society (Orlando, FL; August, 1996).

References

1. A.L. Lafleur, P.A. Monchamp, E.F. Plummer, and M.J. Wornat. Universal calibration method for the determination of polycyclic aromatic hydrocarbons by high performance liquid chromatography with broadband diode-array detection. *Anal. Letters* **20:** 1171–92 (1987).
2. B. Brûlé. Contribution de la chromatographie sur gel perméable à la characterisation qualitative et quantitative des bitumes: Structure colloidale. *Lab. Ponts et Chaussées, Res. Rep.* **76** (1978).
3. S. Coulombe. Comparison of detectors for size exclusion chromatography of heavy oil related samples. *J. Chromatogr. Sci.* **26:** 1–6 (1988).
4. J. Vela, V.L. Cebolla, L. Membrado, and J.M. Andrés. Quantitative hydrocarbon group type analysis of petroleum hydroconversion products using an improved TLC–FID system. *J. Chromatogr. Sci.* **33:** 417–25 (1995).
5. J.M. Charlesworth. Evaporative analyzer as a mass detector for liquid chromatography. *Anal. Chem.* **50:** 1414–20 (1978).
6. T.H. Mourey and L.E. Oppenheimer. Principles of operation of an evaporative light-scattering detector for liquid chromatography. *Anal. Chem.* **56:** 2427–34 (1984).
7. A. Stolyhwo, H. Colin, and G. Guiochon. Use of light scattering as a detector principle in liquid chromatography. *J. Chromatogr.* **265:** 1–18 (1983).
8. A. Stolyhwo, H. Colin, M. Martin, and G. Guiochon. Study of the qualitative and quantitative properties of the light scattering detector. *J. Chromatogr.* **288:** 253–75 (1984).
9. J. Bécart, C. Chevalier, and J.P. Biesse. Quantitative analysis of phospholipids by HPLC with a light scattering evaporating detector. Application to raw materials for cosmetic use. *J. High Res. Chromatogr.* **13:** 126–29 (1990).
10. P. Van der Meeren, J. Vanderdeelen, and L. Baert. Simulation of the mass response of the evaporative light scattering detector. *Anal. Chem.* **64:** 1056–62 (1992).
11. M. Dreux, M. Lafosse, L. Morin-Allory. The evaporative light scattering detector. A universal instrument for non-volatile solutes in LC and SFC. *LC–GC Int.* **9:** 146–55 (1996).
12. M. Lafosse, C. Elfakir, L. Morin-Allory, and M. Dreux. The advantages of evaporative light scattering detection in pharmaceutical analysis by high performance liquid chromatography and supercritical fluid chromatography. *J. High Res. Chromatogr.* **15:** 312–18 (1992).
13. P.A. Asmus and J.B. Landis. Analysis of steroids in bulk pharmaceuticals by liquid chromatography with light scattering detection. *J. Chromatogr.* **316:** 461–64 (1984).
14. ELSD-MK IIA Varex evaporative light-scattering detector. Varex Corporation, 4000 Blackburn Lane, Burtonsville, MD 20866.
15. K.D. Bartle, N. Taylor, M.J. Mulligan, D.G. Mills, and C. Gibson. Evaporative analyzer as a mass detector in the size-exclusion chromatography of coal extracts. *Fuel* **62:** 1181–85 (1983).
16. J.W. Larsen and Y.C. Wei. Macromolecular chemistry of coalification. Molecular weight distribution of pyridine extracts. *Energy & Fuels* **2:** 344–50 (1988).
17. M. Nishioka and J.W. Larsen. Mild pyrolytic production of low molecular weight compounds from high molecular weight coal extracts. *Energy & Fuels* **2:** 351–55 (1988).
18. B.R. Johnson, K.D. Bartle, A.A. Herod, and R. Kandiyoti. Improved size exclusion chromatography of coal-derived materials using *N*-methyl-2-pyrrolidinone as mobile phase. *Prepr. Am. Chem. Soc., Div. of Fuel Chem.* **40 (3):** 457–60 (1995).
19. E. Meehan and S. Oakley. A 3-µm polymeric packing material for gel permeation chromatography. *LC–GC Intl.* **5:** 32–37 (1993).
20. R.P.W. Scott. *Quantitative Analysis using Chromatographic Techniques.* E. Katz, Ed. Separation Science Series. John Wiley & Sons, New York, NY, 1987, ch. 1, p. 24.
21. F. Zarrin, J.A. Risfelt, and N.J. Dovichi. Light scattering detection within the sheath flow cuvette for size determination of multicomponent submicrometer particle suspensions. *Anal. Chem.* **59:** 850–54 (1987).
22. M. Kerker. *The Scattering of Light and Other Electromagnetic Radiation,* 2nd ed. Academic Press, New York, NY, 1969.
23. M. Dreux, M. Lafosse. Mesure de la diffusion de la lumière sur des microparticules en phase gazeuse. Utilisations actuelles. Perspectives. *Analusis* **20:** 587–95 (1992).
24. T.H. Mourey and L.E. Oppenheimer. Principles of operation of an evaporative light scattering detector for liquid chromatography. *Anal. Chem.* **56:** 2427–34 (1984).
25. M. Righezza and G. Guiochon. Effects of the nature of the solvent and solutes on the response of a light scattering detector. *J. Liquid Chromatogr.* **11:** 1967–2004 (1988).

Manuscript accepted November 13, 1996.